hibited, but with a similar rate of chloro hydrolyses compared to cisplatin, this would lead to species with improved antitumor properties and lower toxicities.

The promising antitumor activities of the new platinum complexes with general formulas [Pt(diam)(R'R''SO)Cl](NO_3) (diam = bidentate amine and R'R''SO = substituted sulfoxide)[23] and [*cis*-Pt(NH_3)$_2$(N-het)Cl]Cl (N-het = heterocyclic amine)[24] could in view of the above have favorable nitrogen over sulfur binding ratios. In conclusion, important information is presented that could ultimately lead to new antitumor complexes such that the binding to sulfur-containing biomolecules is inhibited. This could lead to lower amounts of inactivation and diminished toxic side effects.

Acknowledgment. This study was supported in part by the Netherlands Foundation of Chemical Research (SON) with financial aid from the Netherlands Organization for the Advancement of Research (NWO) through Grant No. 333-17. We are indebted to Johnson Matthey Chemicals Ltd. (Reading, England) for their generous loan of K_2PtCl_4. We acknowledge EC support (Grant No. ST2J-0462-C) allowing regular scientific exchange with the group of Prof. Dr. J. C. Chottard (Paris). Dr. K. Inagaki (Nagoya City University, Nagoya, Japan) and Prof. Dr. R. van Eldik (Witten, BRD) are thanked for a careful reading of the manuscript and for many useful suggestions. The fellowship for M.D. was paid in part by the U.S.-Yugoslav Joint Fund for Scientific and Technological Cooperation in cooperation with the National Science Foundation under Grant No. 8818818 and in part by the Serbian Research Fund.

(23) Farrell, N.; Kiley, D. M.; Schmidt, W.; Hacker, M. P. *Inorg. Chem.* **1990**, *29*, 397.
(24) Hollis, L. S.; Amundsen, A. R.; Stern, E. W. *J. Med. Chem.* **1989**, *32*, 128.

Contribution from the Department of Chemistry, Pohang Institute of Science and Technology, P.O. Box 125, Pohang, 790-330 South Korea, and School of Chemical Sciences, University of Illinois at Urbana-Champaign, Urbana, Illinois 61801

Synthesis and Structure of Transition-Metal Bis(porphyrinato) Complexes. Characterization of $Zr(TPP)_2$ and $Zr(OEP)_2$

Kimoon Kim,*[†] Won S. Lee,[†] Hee-Joon Kim,[†] Sung-Hee Cho,[†] Gregory S. Girolami,*[‡] Philip A. Gorlin,[‡] and Kenneth S. Suslick*[‡]

Received October 22, 1990

Treatment of $Zr(NEt_2)_4$ with the free-base porphyrins 5,10,15,20-tetraphenylporphyrin (H_2TPP) or 2,3,7,8,12,13,17,18-octaethylporphyrin (H_2OEP) gives the transition-metal bis(porphyrinato) complexes $Zr(TPP)_2$ and $Zr(OEP)_2$. The hafnium analogue $Hf(OEP)_2$ may be prepared similarly from $Hf(NEt_2)_4$. The complexes have been characterized by UV-vis and ^1H NMR spectroscopy, and the molecular structure of $Zr(TPP)_2$ has been determined crystallographically. The Zr-N distances of 2.40 (1) Å and the porphyrin-porphyrin interplanar spacing of 2.56 Å are the shortest such distances in all known M(porphyrinato)$_2$ complexes. The cyclic voltammograms indicate that $Zr(TPP)_2$ and $Zr(OEP)_2$ each undergo two oxidations and two reductions; the redox potentials suggest that there is significant overlap between the π-systems of the two porphyrin rings. Chemical oxidation of the Zr(porphyrinato)$_2$ complexes with phenoxathiinylium hexachloroantimonate has led to the isolation of the π-radical-cation complexes [$Zr(TPP)_2^+$][$SbCl_6^-$] and [$Zr(OEP)_2^+$][$SbCl_6^-$]. The UV-vis, near-IR, EPR, and IR spectra of these cations are consistent with oxidation of the porphyrin-porphyrin π-system; most notable are the unusually high energy near-IR bands at 1110 and 962 nm in the TPP and OEP complexes, respectively. The high energy of these bands with respect to those of other [M(porphyrinato)$_2^+$] cations with larger metal atoms again can be rationalized on the basis of unusually strong overlap between the π-systems of the two porphyrin rings. Crystallographic data for $Zr(TPP)_2 \cdot C_5H_{12}$: monoclinic, space group $C2/c$, with a = 21.183 (3) Å, b = 21.263 (4) Å, c = 18.688 (3) Å, β = 124.57 (1)°, V = 6930.9 Å^3, Z = 4; R_F = 0.077 and R_{wF} = 0.083 for 1578 independent reflections with $I > 3\sigma(I)$.

Introduction

Complexes that possess two phthalocyanine[1] or two porphyrin[2] macrocycles bound to a single metal center are proving useful as structural and spectroscopic models of the bacteriochlorophyll special pair in the reaction center[3] of photosynthesis. To date, such bis(porphyrinato)metal complexes have only been prepared with metals that possess very large ionic radii (>1.0 Å) such as yttrium,[4] the lanthanides,[5] and the actinides (U and Th).[6] We now report the synthesis, characterization, and X-ray structure of *transition-metal* bis(porphyrinato) complexes, $Zr(TPP)_2$ and $Zr(OEP)_2$.[7] In these compounds, the two porphyrin rings are held in unusually close proximity due to the smaller ionic radius of zirconium (ca. 0.84 Å). These complexes exhibit interesting and unusual properties as a result of the small distance between the two porphyrin ring planes.

Results and Discussion

The preparation of the bis(porphyrinato)zirconium and -hafnium complexes follows our previously described synthesis of the thorium and uranium analogues.[6] Thus, treatment of the diethylamido complex[8] $Zr(NEt_2)_4$ with the free porphyrins H_2TPP and H_2OEP, followed by chromatography on alumina or silica gel, yields $Zr(TPP)_2$ and $Zr(OEP)_2$ in 54% and 55% yields, re-

[†] Pohang Institute of Science and Technology.
[‡] University of Illinois at Urbana-Champaign.

(1) (a) Kirin, I. S.; Moskalev, P. N. *Russ. J. Phys. Chem.* (*Eng. Transl.*) **1967**, *41*, 251. (b) Moskalev, P. N.; Kirin, I. S. *Russ. J. Phys. Chem.* (*Engl. Transl.*) **1972**, 46, 1019-1022. (c) Walton, D.; Ely, B.; Elliot, G. *J. Electrochem. Soc.* **1981**, *128*, 2479-2484. (d) Andre, J. J.; Simon, J.; Even, R.; Boudjema, B.; Guillaud, G.; Maitrot, M. *Synth. Met.* **1987**, *18*, 683-688. (e) Tomilova, L. G.; Ovchinnikova, N. A.; Luk'yanets, E. A. *Zh. Obshch. Khim.* **1987**, *57*, 2100-2103. (f) Silver, J.; Lukes, P. J.; Key, P. K.; O'Connor, J. M. *Polyhedron* **1989**, *8*, 1631-1635. (g) Ercolani, C.; Paoletti, A. M.; Pennesi, G.; Rossi, G.; Chiesi-Villa, A.; Rizzoli, C. J. *Chem. Soc., Dalton Trans.* **1990**, 1971-1977.
(2) (a) Buchler, J. W.; Elsässer, K.; Kihn-Botulinski, M.; Scharbert, B. *Angew. Chem., Int. Ed. Engl.* **1986**, *25*, 286-287. (b) Buchler, J. W.; Scharbert, B. *J. Am. Chem. Soc.* **1988**, *110*, 4272-4276. (c) Bilsel, O.; Rodriguez, J.; Holten, D., Girolami, G. S.; Milam, S. N.; Suslick, K. S. *J. Am. Chem. Soc.* **1990**, *112*, 4075-4077.
(3) For a review, see: Deisenhofer, J.; Michel, H. *Science* **1989**, *245*, 1463-1473.
(4) (a) Buchler, J. W.; Huttermann, J.; Loffler, J. *Bull Chem. Soc. Jpn.* **1988**, *61*, 71-77. (b) We are aware of parallel studies on Zr(porph)$_2$ complexes: Buchler, J. W.; De Cian, A.; Fischer, J.; Hammerschmitt, P.; Weiss, R. *Chem. Ber.*, in press.
(5) (a) Buchler, J. W.; Kapellmann, H.-G.; Knoff, M.; Lay, K.-L.; Pfeifer, S. *Z. Naturforsch.* **1983**, *38B*, 1339-1345. (b) Buchler, J. W.; De Cian, A.; Fischer, J.; Kihn-Botulinski, M.; Paulus, H.; Wiess, R. *J. Am. Chem. Soc.* **1986**, *108*, 3652-3659. (c) Buchler, J. W.; De Cian, A.; Fischer, J.; Kihn-Botulinski, M.; Wiess, R. *Inorg. Chem.* **1988**, *27*, 339-345.

0020-1669/91/1330-2652$02.50/0

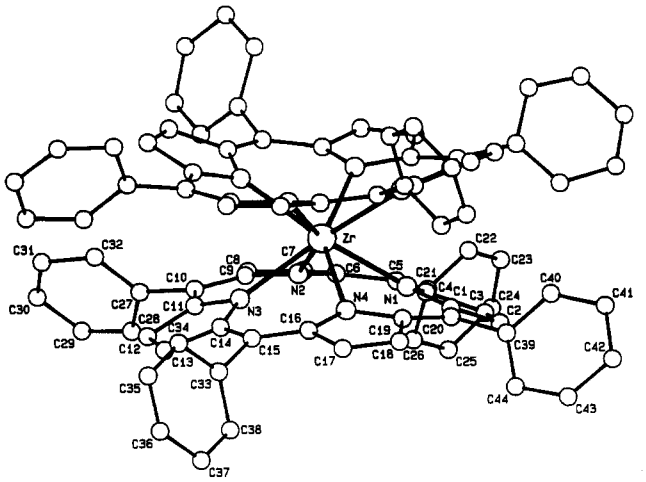

Figure 1. Molecular structure of $Zr(TPP)_2$. The average Zr–N bond distance is 2.40 (1) Å; the two porphyrin N_4 mean planes are 2.56 Å apart and describe a twist angle of 37°; the two 24-atom mean planes are 3.29 Å apart.

Table I. Crystallographic Data for $Zr(TPP)_2 \cdot C_5H_{12}$

formula	$ZrN_8C_{88}H_{56} \cdot C_5H_{12}$
fw	1388.85
space group	$C2/c$ (No. 15)
a, Å	21.183 (3)
b, Å	21.263 (4)
c, Å	18.688 (3)
β, deg	124.57 (1)
V, Å^3	6930.9
Z	4
temp, °C	23
d(measd), g/cm^3	1.34
d(calcd), g/cm^3	1.331
cryst size, mm	0.20 × 0.20 × 0.22
radiation	graphite-monochromated Mo Kα (λ(Kα_1) = 0.7093 Å)
linear abs coeff, cm^{-1}	2.1
scan mode	ω scan
scan speed, deg/min	2.06; for reflns with $I < 3\sigma(I)$, rescans forced to achieve $I > 3\sigma(I)$, up to 60 s total scan time
2θ limits, deg	$6.0 \le 2\theta \le 44.0$
bkgd counts	$^1/_4$ scan range on each side of refln
scan width, deg	0.7 in ω
no. of unique data	3369
no. of unique data with $I > 3\sigma(I)$	1578
no. of variables	238
R_F	0.077
R_{wF}	0.083
GOF	1.21

spectively. The hafnium analogue $Hf(OEP)_2$ may be prepared similarly from $Hf(NEt_2)_4$. As is typical for bis(porphyrinato) metal complexes, the Soret bands (396 nm for $Zr(TPP)_2$ and 381 nm for $Zr(OEP)_2$) are blue-shifted with respect to analogous mono(porphyrinato) species; in addition, the Soret bands in both complexes have a moderately intense shoulder at shorter wavelengths (at 348 nm in $Zr(TPP)_2$ and at 355 nm in $Zr(OEP)_2$). Thus, the Soret band is split into two components. The ^{1}H NMR spectra of $Zr(TPP)_2$ and $Zr(OEP)_2$ are similar to those of the corresponding cerium(IV) and thorium(IV) complexes.[6b,9] The ^{1}H NMR and UV–vis spectra of $Hf(OEP)_2$ are essentially identical with those of $Zr(OEP)_2$.

Table II. Positional and Equivalent Isotropic Thermal Parameters for $Zr(TPP)_2 \cdot C_5H_{12}$[a]

atom	x	y	z	B_{eq}, Å^2
Zr	0.000	0.12502 (9)	0.750	2.23 (5)
N1	−0.1321 (5)	0.0950 (4)	0.6660 (7)	2.1 (3)
N2	−0.0098 (5)	0.0343 (4)	0.6672 (7)	2.2 (3)
N3	0.0478 (5)	0.1547 (4)	0.6665 (6)	2.2 (3)
N4	−0.0726 (5)	0.2155 (4)	0.6667 (7)	2.7 (3)
C1	−0.1932 (6)	0.1334 (6)	0.6447 (8)	2.5 (3)
C2	−0.2621 (7)	0.0954 (6)	0.610 (1)	3.8 (3)
C3	−0.2441 (7)	0.0350 (6)	0.6063 (9)	3.5 (3)
C4	−0.1638 (7)	0.0349 (6)	0.6382 (8)	2.7 (3)
C5	−0.1270 (6)	−0.0176 (6)	0.6399 (8)	2.6 (3)
C6	−0.0550 (6)	−0.0177 (6)	0.6522 (8)	2.9 (3)
C7	−0.0222 (7)	−0.0715 (6)	0.6407 (9)	3.3 (3)
C8	0.0407 (7)	−0.0536 (6)	0.6448 (9)	3.0 (3)
C9	0.0459 (7)	0.0127 (6)	0.6589 (8)	2.5 (3)
C10	0.0953 (7)	0.0514 (6)	0.6496 (9)	3.0 (3)
C11	0.0891 (7)	0.1175 (6)	0.6440 (8)	3.1 (3)
C12	0.1219 (7)	0.1538 (6)	0.6084 (9)	3.1 (3)
C13	0.0981 (7)	0.2139 (6)	0.6054 (9)	3.7 (3)
C14	0.0533 (7)	0.2156 (6)	0.6409 (9)	2.8 (3)
C15	0.0154 (7)	0.2688 (6)	0.6403 (8)	2.6 (3)
C16	−0.0422 (7)	0.2674 (6)	0.6515 (9)	2.8 (3)
C17	−0.0883 (7)	0.3221 (6)	0.6400 (9)	3.2 (3)
C18	−0.1473 (7)	0.3022 (6)	0.6441 (9)	3.2 (3)
C19	−0.1387 (6)	0.2356 (5)	0.6595 (8)	2.4 (3)
C20	−0.1940 (7)	0.1990 (6)	0.6506 (8)	2.6 (3)
C21	−0.1731 (7)	−0.0781 (6)	0.6079 (9)	3.6 (3)
C22	−0.1912 (8)	−0.1078 (7)	0.659 (1)	4.6 (4)
C23	−0.2383 (9)	−0.1626 (8)	0.627 (1)	5.6 (4)
C24	−0.2665 (9)	−0.1813 (8)	0.547 (1)	6.0 (4)
C25	−0.249 (1)	−0.1542 (8)	0.491 (1)	6.5 (5)
C26	−0.1976 (9)	−0.1000 (7)	0.524 (1)	5.5 (4)
C27	0.1514 (7)	0.0210 (6)	0.6366 (9)	3.0 (3)
C28	0.1271 (8)	−0.0183 (7)	0.563 (1)	4.2 (3)
C29	0.1795 (8)	−0.0472 (7)	0.556 (1)	4.9 (4)
C30	0.2554 (9)	−0.0361 (8)	0.611 (1)	5.7 (4)
C31	0.2804 (9)	0.0032 (7)	0.678 (1)	5.4 (4)
C32	0.2287 (9)	0.0328 (7)	0.694 (1)	5.4 (4)
C33	0.0321 (7)	0.3283 (6)	0.6067 (9)	3.2 (3)
C34	0.1012 (8)	0.3571 (6)	0.660 (1)	4.4 (4)
C35	0.1147 (9)	0.4115 (8)	0.627 (1)	5.9 (4)
C36	0.0616 (9)	0.4318 (8)	0.548 (1)	5.9 (4)
C37	−0.0086 (9)	0.4028 (8)	0.493 (1)	6.0 (4)
C38	−0.0224 (8)	0.3495 (6)	0.524 (1)	4.2 (4)
C39	−0.2646 (7)	0.2283 (6)	0.6347 (9)	3.4 (3)
C40	−0.2853 (8)	0.2170 (7)	0.691 (1)	4.2 (3)
C41	−0.352 (1)	0.2444 (8)	0.682 (1)	6.4 (5)
C42	−0.3959 (9)	0.2867 (7)	0.612 (1)	5.5 (4)
C43	−0.3745 (8)	0.2973 (7)	0.556 (1)	4.0 (3)
C44	−0.3108 (8)	0.2675 (7)	0.564 (1)	4.2 (3)
C45	0.000	0.523 (3)	0.250	8 (1)
C46	0.039 (2)	0.495 (2)	0.341 (2)	5.3 (9)
C47	−0.982 (2)	0.456 (2)	0.182 (3)	39 (1)
C48	0.034 (5)	0.297 (4)	0.328 (6)	19 (3)
C49	0.055 (2)	0.254 (2)	0.343 (2)	6.1 (9)
C50	0.000	0.230 (4)	0.250	13 (2)

[a] For anisotropically refined atoms (Zr and four N atoms), the table lists the isotropic equivalent displacement parameter (B_{eq}) defined as $(4/3)[a^2B(1,1) + b^2B(2,2) + c^2B(3,3) + ab(\cos\gamma)B(1,2) + ac(\cos\beta)B(1,3) + bc(\cos\alpha)B(2,3)]$.

The structure of $Zr(TPP)_2 \cdot C_5H_{12}$ has been determined by X-ray crystallography; the crystals are isomorphous with those of the previously described[6b] thorium analogue $Th(TPP)_2 \cdot C_7H_8$ (although the refinement was carried out in a different monoclinic setting). The $Zr(TPP)_2$ molecule resides on a crystallographic 2-fold axis that passes through the zirconium atom (Figure 1). The Zr^{IV} center is coordinated to the eight nitrogen atoms of the two porphyrin rings in a distorted square-antiprismatic arrangement. The average Zr–N bond distance is 2.40 (1) Å, and the displacement of the zirconium atom from each of the porphyrin N_4 planes is 1.28 Å (cf. Tables III and IV). The two N_4 mean planes are 2.56 Å apart, the two 24-atom mean planes are 3.29 Å apart, and the two porphyrin macrocycles are twisted with respect to

(6) (a) Girolami, G. S.; Milam, S. N.; Suslick, K. S. *Inorg. Chem.* **1987**, *26*, 343–344. (b) Girolami, G. S.; Milam, S. N.; Suslick, K. S. *J. Am. Chem. Soc.* **1988**, 110, 2011–2012.
(7) Abbreviations: TPP, 5,10,15,20-tetraphenylporphyrinate(2–); OEP, 2,3,7,8,12,13,17,18-octaethylporphyrinate(2–).
(8) (a) Bradley, D. C.; Thomas, I. M. *J. Chem. Soc.* **1960**, 3857–3861. (b) Chandra, G.; Lappert, M. F. *J. Chem. Soc. A* **1968**, 1940–1945.
(9) Buchler, J. W.; De Cian, A.; Fischer, J.; Hammerschmitt, P.; Loffler, J.; Scharbert, B.; Weiss, R. *Chem. Ber.* **1989**, *122*, 2219–2228.

Table III. Selected Bond Lengths (Å) and Angles (deg) in $Zr(TPP)_2 \cdot C_5H_{12}$

	Bond Lengths		
Zr–N1	2.392 (9)	Zr–N3	2.38 (1)
Zr–N2	2.41 (1)	Zr–N4	2.402 (9)
	Bond Angles		
N1–Zr–N2	73.9 (4)	N1–Zr–N4	73.0 (3)
N2–Zr–N3	72.8 (3)	N1–Zr–N3	114.6 (3)
N2–Zr–N4	73.6 (4)	N2–Zr–N4	115.8 (4)

Table IV. Comparison of Structural Features[a] of $Zr(TPP)_2$, $Th(TPP)_2$, and $Th(TPP)_2^+$

	$Zr(TPP)_2$	$Th(TPP)_2$	$Th(TPP)_2^+$
av M–N, Å	2.40 (1)	2.55 (1)	2.52 (2)
$M–Ct_N$, Å	1.28	1.47	1.45
$M–Ct_P$, Å	1.64	1.76	1.67
doming, Å	0.36	0.29	0.22
$Ct_N–Ct_N$, Å	2.56	2.89	2.89
$Ct_P–Ct_P$, Å	3.29	3.47	3.33
inter-porphyrin twist, deg	37	31	30
M ionic radius, Å	0.84	1.05	1.05

[a] $M–Ct_N$: metal displacement from mean N_4 plane. $M–Ct_P$: metal displacement from mean 24-atom porphyrin plane. Doming = $(M–Ct_P) - (M–Ct_N)$. Ct–Ct: interplanar spacing. The parameters for the Th complexes are from ref 6b.

each other by about 37°. The structural parameters are compared with those[6b] of $Th(TPP)_2$ and $[Th(TPP)_2^+][SbCl_6^-]$ in Table IV. The greater extent of porphyrin doming for $Zr(TPP)_2$ versus $Th(TPP)_2$ (0.36 Å vs 0.29 Å, respectively) reflects the smaller ionic radius[10] of Zr^{IV} (0.84 Å) versus Th^{IV} (1.05 Å). $Zr(TPP)_2$ has the shortest known interporphyrin distance among the sandwich-type porphyrin complexes.[5b,5c,6b,9]

The doming of porphyrin skeleton is illustrated by the deviations of atoms from the least-squares plane of the 24-atom porphyrin core (Figure 2). The average deviation is 0.21 Å, and particularly large deviations are observed in the pyrrole rings of "N1" and "N3". The large deformation of the porphyrin core is also indicated by the large dihedral angles between the four pyrrole rings and the mean porphyrin plane: 23.1, 9.9, 24.2, 10.0°. Least-squares planes and dihedral angles between the least-squares planes are listed in the supplementary material. The individual pyrrole rings are essentially planar. The bond distances and angles of the porphyrin core are close to the values typical of metalloporphyrins.[11]

The electrochemical behavior of $Zr(TPP)_2$ and $Zr(OEP)_2$ has been studied by cyclic voltammetry. The TPP compound undergoes two reversible one-electron oxidations at 0.62 and 1.05 V vs Ag/AgCl and two reversible one-electron reductions at −1.23 and −1.59 V vs Ag/AgCl. The OEP compound shows two reversible oxidations at 0.551 and 0.062 V in CH_2Cl_2 (0.77 and 0.29 V in THF) and two irreversible reductions in THF at roughly −1.4 and −1.7 V vs Ag/AgCl. The oxidation potentials of $Zr(TPP)_2$ are nearly the same as those of $Th(TPP)_2$,[6b] $U(TPP)_2$,[6b] and $Ce(TPP)_2$,[9] but this is not true for the OEP compounds. The +2/+1 and +1/0 redox potentials show that $Zr(OEP)_2$ is easier to oxidize than the corresponding $Th(OEP)_2$ ($E_{1/2}$ = 0.91 and 0.48 V) and $U(OEP)_2$ ($E_{1/2}$ = 0.82 and 0.40 V) complexes. This behavior suggests that, in all three $M(OEP)_2$ complexes, the HOMO is antibonding between the two porphyrin π-systems.[2,12]

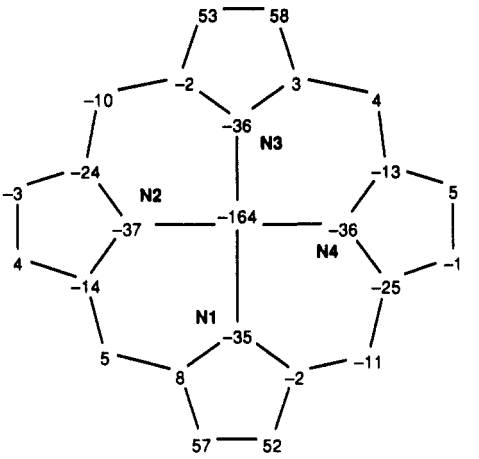

Figure 2. Displacements (in pm) of atoms from the least-squares plane of the 24-atom porphyrin skeleton. The estimated standard deviation is ca. 1 pm.

Treatment of the bis(porphyrinato)zirconium complexes with 1.1 equiv of phenoxathiinylium hexachloroantimonate in CH_2Cl_2, followed by crystallization from CH_2Cl_2/hexanes or CH_2Cl_2/toluene, produces the radical-cation complexes $[Zr(TPP)_2][SbCl_6]$ and $[Zr(OEP)_2][SbCl_6]$ in 62% and 42% yields, respectively. The Soret bands of the oxidized compounds are shifted to higher energy (376 nm for the TPP complex and 356 nm for the OEP complex) compared to the bands of the neutral precursors. The EPR spectrum of $[Zr(TPP)_2][SbCl_6]$ in CH_2Cl_2 at 96 K exhibits a signal at g = 2.009 (line width = 5.75 G), and the EPR spectrum of $[Zr(OEP)_2][SbCl_6]$ is very similar except the line width is even narrower (g = 2.006 and line width = 1.9 G at 115 K). Both of these signals confirm that oxidation of the bis(porphyrinato)-zirconium complexes removes one electron from the π-system of the porphyrin rings. The π-cation-radical nature of the compounds is also supported by the presence of radical-cation "marker" bands[13] at 1319 and at 1556 cm^{-1} in the IR spectra of $[Zr(TPP)_2][SbCl_6]$ and $[Zr(OEP)_2][SbCl_6]$, respectively.

The cationic bis(porphyrinato)zirconium complexes both show a broad absorption in the near-IR spectrum at 1110 nm (fwhm = 200 nm) for $[Zr(TPP)_2][SbCl_6]$ and at 962 nm (fwhm = 130 nm) for $[Zr(OEP)_2][SbCl_6]$. Similar near-IR absorptions have been observed for other metal bis(porphyrinato) sandwich complexes that have π-cation-radical character.[2,5,6] There is a direct correlation[6b,2] between the energy of the $[M(porphyrinato)_2^+]$ near-IR band and the ionic radius of the central metal, which is extended by the zirconium complexes described here: $[Zr(OEP)_2^+]$ and $[Zr(TPP)_2^+]$ have the highest energy absorption bands in near-IR region of all the known metal porphyrin sandwich complexes, which is consistent with the fact that these zirconium complexes have the shortest interporphyrin distances.

Conclusions

The transition-metal bis(porphyrinato) complexes $Zr(TPP)_2$ and $Zr(OEP)_2$, their monocations, and their hafnium analogues have been synthesized and fully characterized. The molecular structure of $Zr(TPP)_2$ has been determined crystallographically and shows that this molecule possesses the shortest known porphyrin–porphyrin interplanar spacing. Chemical oxidation of the neutral complexes leads to the isolation of salts of the π radical cations $Zr(TPP)_2^+$ and $Zr(OEP)_2^+$. In these cations, near-infrared absorptions are observed that have the highest energy of all metalloporphyrin sandwich complexes, consistent with the very strong interporphyrin π interactions. We are continuing to explore the chemical and physical consequences of the extremely short interporphyrin distances in these complexes.

(10) Shannon, R. D. *Acta Crystallogr.* **1976**, *A32*, 751–767.
(11) (a) Scheidt, W. R.; Lee, Y. J. *Struct. Bonding (Berlin)* **1987**, *67*, 1–70. (b) Scheidt, W. R. In *The Porphyrins*; Dolphin, D., Ed.; Academic Press: New York, 1978; Vol. III, pp 463–512. (c) Hoard, J. L. In *Porphyrins and Metalloporphyrins*; Smith, K. M., Ed.; Elsevier: Amsterdam, 1975; pp 317–380.
(12) (a) Yan, X.; Holten, D. *J. Phys. Chem.* **1988**, *92*, 409–414. (b) Donohoe, R. J.; Duchowski, J. K.; Bocian, D. F. *J. Am. Chem. Soc.* **1988**, *110*, 6119–6124. (c) Duchowski, J. K.; Bocian, D. F. *J. Am. Chem. Soc.* **1990**, *112*, 3312–3318.
(13) Shimomura, E. T.; Phillippi, M. A.; Goff, H. M.; Scholz, W. F.; Reed, C. A. *J. Am. Chem. Soc.* **1981**, *103*, 6778–6780.

Experimental Section

Chemicals. All chemicals were of reagent grade and were used without further purification except as noted below. Argon was purified by passage through successive columns of activated molecular sieves 13X (Aldrich) and Ridox (Fisher). H_2TPP, H_2OEP, and phenoxathiinylium hexachloroantimonate were prepared by literature procedures.[14] All solvents were distilled from their sodium benzophenone ketyl solutions (toluene, ether, and hexanes) or from CaH_2 or P_2O_5 (CH_2Cl_2) under an atmosphere of nitrogen. The supporting electrolyte, tetrabutylammonium perchlorate (TBAP) (Fluka), was recrystallized twice from ethanol.

Methods and Instruments. All manipulations of oxygen- and water-sensitive materials were performed either in a Vacuum/Atmospheres glovebox under a nitrogen atmosphere or in Schlenkware under an atmosphere of purified Ar. UV–visible spectra were recorded on an Hewlett-Packard 8452A spectrophotometer. ^1H NMR spectra were obtained from a Bruker AM-300 or a Nicolet NT360 spectrometer. High-resolution mass spectra were obtained on a VG70-250SE mass spectrometer (VG Analytical). Fourier transform infrared and near-infrared spectra were obtained on a Bomen DA3.01 or a Perkin-Elmer 1650 spectrophotometer. Other near-IR spectra were obtained on a Varian 2300 spectrophotometer. EPR spectra were recorded in frozen CH_2Cl_2 at 96 K on a Bruker ER 200D-SRC or ESP-300 spectrometer.

Electrochemical experiments were performed with a Bioanalytical BAS 100 or a Pine Instrument RDE4 bipotentiostat. Cyclic voltammetry was carried out with standard three-electrode cells. A platinum-button electrode was used as the working electrode, a platinum wire as the counter electrode, and a silver wire as the pseudoreference electrode. Cyclic voltammograms were obtained on approximately 5×10^{-4} M solutions of the samples in 0.2 M TBAP in CH_2Cl_2 or in some cases in tetrahydrofuran. Ferrocene was added as an internal standard ($Cp_2Fe^{+/0}$) = 0.40 V vs Ag wire). To maintain an O_2-free environment, the solution was blanketed with nitrogen during experiments.

Syntheses. (a) Tetrakis(diethylamido)zirconium(IV), $Zr(NEt_2)_4$. This reaction was carried out under argon by using standard Schlenk techniques. $Zr(NEt_2)_4$ was made according to the literature route with some modification.[8a] $ZrCl_4$ (1.60 g, 6.80 mmol) and $LiNEt_2$ (2.28 g, 28.8 mmol) were combined in a Schlenk flask equipped with a magnetic stirring bar. Diethyl ether (120 mL) was added, and the mixture was stirred for 24 h. The pale gray solution was filtered from some insoluble salts, and the ether was removed under vacuum. The yellow residue was extracted with pentane (30 mL) and the extract filtered from a small amount of insoluble salts. The pentane was then removed under vacuum to give $Zr(NEt_2)_4$ as a pale yellow liquid, which was used without further purification. Yield: 1.20 g (67%).

(b) Bis(5,10,15,20-tetraphenylporphyrinato)zirconium(IV), $Zr(TPP)_2$. The reaction was carried out by using Schlenk techniques under an atmosphere of purified argon. H_2TPP (216 mg, 0.352 mmol) was dissolved in toluene (ca. 20 mL), and the mixture was heated. To the refluxing solution was added $Zr(NEt_2)_4$ (1.40 g, 3.69 mmol), and the resultant mixture was refluxed for 18 h. The progress of the reaction was monitored by UV–vis spectroscopy and TLC. After 18 h, the reaction mixture was allowed to cool to room temperature, and the solvent was removed in vacuo. The residue was chromatographed through an alumina column (Grade I, basic, Fluka, 2.5 × 8 cm) with toluene. The first orange-red band [$Zr(TPP)_2$] was collected and the fraction evaporated to dryness under reduced pressure at room temperature. The crude product was recrystallized from CH_2Cl_2/pentane to yield 125 mg of $Zr(TPP)_2$ (54%). Anal. Calcd for $C_{88}H_{56}N_8Zr \cdot CH_2Cl_2$: C, 76.3; H, 4.18; N, 8.00. Found: C, 75.6; H, 4.24; N, 8.06. UV–vis (CH_2Cl_2, nm): λ_{max} (log ϵ) 348 (4.71), 396 (5.59), 422 (sh, 4.55), 451 (sh, 4.27), 506 (4.44), 551 (4.01), 692 (3.25). ^1H NMR (300 MHz, CD_2Cl_2, −20 °C): δ 9.22 (d, J_{HH} = 7.3 Hz, *o*-H), 8.27 (s, pyrrole H), 8.13 (dd, J_{HH} = 7.4, 7.3 Hz, *m*-H), 7.73 (dd, J_{HH} = 7.4, 7.4 Hz, *p*-H), 7.22 (dd, J_{HH} = 7.3, 7.4 Hz, *m*-H), 6.26 (d, J_{HH} = 7.3 Hz, *o*-H). IR (KBr, cm^{-1}): 3055 (w), 2253 (w), 1813 (w), 1597 (m), 1539 (w), 1489 (m), 1443 (w), 1335 (s), 1223 (w), 1180 (w), 1076 (m), 980 (s), 802 (s), 752 (s), 702 (s). High-resolution mass spectrum (LSIMS): m/z 1315.3749, calcd for $C_{88}H_{57}N_8Zr$ (MH^+) 1315.3753.

(c) Bis(5,10,15,20-tetraphenylporphyrinato)zirconium(IV) Hexachloroantimonate, [$Zr(TPP)_2$][$SbCl_6$]. A solution of $Zr(TPP)_2$ (7.5 mg, 5.70 μmol) in CH_2Cl_2 (ca. 10 mL) was treated with 1.1 equiv of phenoxathiinylium hexachloroantimonate. The process was accompanied by a color change from orange-red to red-brown and monitored by UV–vis spectroscopy. After completion of the reaction, the solvent was removed in vacuo. Recrystallization from CH_2Cl_2/pentane or CH_2Cl_2/hexanes yielded 5.7 mg of [$Zr(TPP)_2$][$SbCl_6$] (62%). Anal. Calcd for $C_{88}H_{56}Cl_6N_8SbZr \cdot CH_2Cl_2$: C, 61.6; H, 3.37; N, 6.45. Found: C, 61.0; H, 3.48; N, 6.38. UV–vis (CH_2Cl_2, nm): λ_{max} (log ϵ) 376 (5.00), 548 (4.07). Near-IR (KBr, nm): λ_{max} 1110 (fwhm = 200 nm). IR (KBr, cm^{-1}): 3055 (w), 2280 (w), 1597 (w), 1566 (w), 1489 (s), 1439 (s), 1319 (s), 1219 (w), 1176 (s), 1076 (m), 1003 (m), 972 (s), 876 (w), 806 (s), 698 (s).

(d) Bis(2,3,7,8,12,13,17,18-octaethylporphyrinato)zirconium(IV), $Zr(OEP)_2$. H_2OEP (2.41 g, 4.5 mmol) was added to toluene (150 mL) in a three-neck flask equipped with a reflux condenser, and the mixture was heated to reflux. To the hot solution was added via cannula $Zr(NEt_2)_4$ (0.86 g, 2.25 mmol) dissolved in pentane (20 mL), and reflux was continued. The reaction progress was monitored by UV–vis spectroscopy and refluxing stopped after 44 h. The mixture was allowed to cool slowly to room temperature, and at this time the flask was opened to the atmosphere. The toluene was removed by using a rotary evaporator, and the residue was extracted with pentane (3 × 50 mL). The extracts were combined, filtered, and taken to dryness. The remaining solid residue was separated by column chromatography on silica gel using a 1:1 ratio of toluene and hexane. The bis(porphyrinato) complex eluted first. Yield: 1.42 g (55%). Anal. Calcd for $C_{72}H_{88}N_8Zr$: C, 74.7; H, 7.67; N, 9.68; Zr, 7.89. Found: C, 74.4; H, 7.80; N, 9.54; Zr, 7.63. UV–vis (CH_2Cl_2, nm): 355, 381 (Soret), 483, 547, 589. FD MS: m/z 1157 (MH^+). ^1H NMR (C_6D_6, 25 °C): δ 9.23 (s, meso H), 4.16 (dq, J_{HH} = 7.5, 15 Hz, CH_2), 1.54 (t, J_{HH} = 15 Hz, CH_3). IR (KBr, cm^{-1}): 2964 (s), 2931 (s), 2870 (s), 1466 (sh), 1384 (s), 1269 (m), 1220 (m), 1057 (m), 1015 (s), 955 (s), 915 (w), 840 (m), 687 (m). Crystal data for $Zr(OEP)_2$: monoclinic, space group $P2_1/n$, a = 15.489 (17) Å, b = 15.390 (21) Å, c = 26.210 (30) Å, β = 92.44 (3)°, V = 6348 (7) Å^3; monochromated Mo Kα radiation (λ = 0.71073 Å) on a Syntex $P2_1$ diffractometer. The crystals of Zr(OEP) are isomorphous with those of $Ce(OEP)_2$.[5b]

(e) Bis(2,3,7,8,12,13,17,18-octaethylporphyrinato)zirconium(IV) Hexachloroantimonate, [$Zr(OEP)_2$][$SbCl_6$]. CH_2Cl_2 (35 mL) was added to a mixture of $Zr(OEP)_2$ (0.252 g, 0.218 mmol) and phenoxathiinylium hexachloroantimonate (0.129 g, 0.241 mmol). The solution was stirred for 2 h, filtered, and concentrated to ca. 15 mL. Toluene (50 mL) was added, and the solution was allowed to stand for 12 h. The solution was then filtered to give a purple powder, which was dried under vacuum. Yield: 0.136 g (42%). Anal. Calcd for $C_{72}H_{88}Cl_6N_8SbZr \cdot 2CH_2Cl_2$: C, 53.5; H, 5.58; N, 6.75; Cl, 21.3; Sb, 7.33; Zr, 5.49. Found: C, 53.6; H, 5.47; N, 6.47; Cl, 19.0; Sb, 7.02; Zr, 4.98. UV–vis (CH_2Cl_2, nm): 356 (Soret), 430, 508, 688. Near-IR (CH_2Cl_2, nm): 962 (fwhm = 132 nm). IR (Nujol, cm^{-1}): 1556 (m), 1139 (w), 1128 (w), 1106 (w), 1059 (m), 1016 (m), 980 (w), 954 (m), 856 (w), 845 (w), 692 (w).

(f) Bis(2,3,7,8,12,13,17,18-octaethylporphyrinato)hafnium(IV), $Hf(OEP)_2$. The synthesis is analogous to that of $Zr(OEP)_2$. Anal. Calcd for $C_{72}H_{88}N_8Hf$: C, 69.5; H, 7.13; N, 9.01. Found: C, 69.4; H, 7.17; N, 8.92. UV–vis (CH_2Cl_2, nm): 355, 377 (Soret), 483, 546, 589. FD MS: m/z 1244.7 (MH^+). ^1H NMR (C_6D_6, 25 °C): δ 9.22 (s, meso H), 4.16 (dq, J_{HH} = 7.2, 15 Hz, CH_2), 3.81 (dq, J_{HH} = 7.3, 15 Hz, CH_2), 1.53 (t, J_{HH} = 7.2 Hz, CH_3).

X-ray Crystal Structure Determination. Crystals of $Zr(TPP)_2$ used in this study were grown by slow diffusion of *n*-pentane into a CH_2Cl_2 solution of the compound. A small, dark purple crystal (0.20 × 0.20 × 0.22 mm) was mounted on an Enraf-Nonius CAD4 diffractometer. Unit cell parameters were determined by least-squares refinement of 25 reflections ($8.6 < \theta(MoK\alpha) < 13.3$) that had been automatically centered on the diffractometer. At the beginning, it was incorrectly assumed that the crystals belong to either space group $I4_1/amd$ or $I4_1/a$ of the tetragonal system and the initial data collection was performed accordingly ($+h,+k,+l$). Later, the correct space group was determined to be $I2/a$ of the monoclinic system and further data collection was made ($\pm h,+k,+l$). No systematic changes were observed in the intensities of four standard reflections that were measured every 3 h of X-ray exposure.

All the calculations were carried out with the Enraf-Nonius Structure Determination Package. The intensity data were corrected for Lorentz and polarization effects, and empirical absorption corrections were also applied. The space group $I2/a$ was then transformed to the standard setting, $C2/c$. The structure was solved by Patterson and difference Fourier methods. Refinement of the structure proceeded smoothly, except for problems with the solvate molecule. No thoroughly satisfactory model for the solvate molecule was found. In the best model, the solvate molecule occupies two different sites with half-occupancy for each. For each site, the central carbon atom of the pentane molecule lies on the 2-fold symmetry axis. Large thermal parameters for the terminal carbon atoms (39 and 19 Å^2 for C47 and C48, respectively) clearly indicate the disorder. The structure of the $Zr(TPP)_2$ molecule did not seem to be significantly affected by the disorder. In the final model, owing to the small number of data with $I > 3\sigma(I)$, only zirconium and nitrogen atoms

(14) (a) Paine J. B.; Kirshner, W. B.; Moskowiktz, D. W.; Dolphin, D. *J. Organomet. Chem.* **1976**, *41*, 3857–3860. (b) Gans, P.; Marchon, J.-C.; Reed, C. A.; Regnard, J.-R. *Nouv. J. Chim.* **1981**, *5*, 203–204.

were refined anisotropically. The positions of hydrogen atoms were calculated (C-H = 0.95 Å) and were included as fixed contributions to the structure factors. Each hydrogen atom was assigned an isotropic thermal parameter 1.2 times that of the atom to which it is attached. No solvent hydrogen atoms were included. The final cycle of refinement on F, involving 1578 observations and 238 variables, converged to the agreement indices given in Table I. The final difference electron density map revealed residual electron density (0.19-0.22 e/Å^3) in the vicinity of the solvate molecule. Crystallographic details are summarized in Table I. The positional parameters and equivalent isotropic thermal parameters for non-hydrogen atoms are listed in Table II. Selected bond distances and angles are presented in Table III.

Acknowledgment. We thank the U.S. NIH, the U.S. DOE., the Pohang Institute of Science and Technology, and the Korea Science and Engineering Foundation for support. We also gratefully acknowledge Professor J. A. Ibers of Northwestern University for obtaining high-resolution mass spectra and Dr. S. R. Wilson and Mr. D. Whang for assistance with the X-ray crystallographic data. G.S.G. and K.S.S. are recipients of A. P. Sloan Research Fellowships, G.S.G. acknowledges a Henry and Camille Dreyfus Teacher-Scholar Award, and K.S.S. an NIH Research Career Development Award.

Supplementary Material Available: Tables of anisotropic thermal parameters, complete bond distances and angles, least-squares planes, and dihedral angles (6 pages); a listing of observed and calculated structure factors (8 pages). Ordering information is given on any current masthead page.

Contribution from the Department of Chemistry,
New York University, New York, New York 10003

Models of Amide-Cysteine Hydrogen Bonding in Rubredoxin: Hydrogen Bonding between Amide and Benzenethiolate in $[(CH_3)_3NCH_2CONH_2]_2[Co(SC_6H_5)_4]\cdot{}^1/_2CH_3CN$ and $[(CH_3)_3NCH_2CONH_2][SC_6H_5]$†

Marc Anton Walters,* John C. Dewan, Caroline Min, and Shirley Pinto

Received January 8, 1991

Amide-thiolate hydrogen-bonding interactions are described for the cobalt complex $[(CH_3)_3NCH_2CONH_2]_2[Co(SC_6H_5)_4]\cdot{}^1/_2CH_3CN$ (**1**) and the metal-free salt $[(CH_3)_3NCH_2CONH_2][SC_6H_5]$ (**2**). Complex **1** has a triclinic cell with space group $P\bar{1}$, a = 16.960 (5) Å, b = 17.874 (6) Å, c = 14.184 (6) Å, α = 111.47 (3)°, β = 94.34 (3)°, γ = 70.50 (2)°, and Z = 4. Complex **2** has a monoclinic cell with space group $P2_1/n$, a = 12.847 (9) Å, b = 6.730 (5) Å, c = 29.268 (4) Å, β = 95.65 (2)°, and Z = 8. Compound **1** serves to model amide-cysteine hydrogen bonding and its effect on metal coordination in rubredoxin. Average N-H···S hydrogen bond lengths are 3.356 (7) and 3.306 (3) Å for **1** and **2**, respectively. In **1** the average Co-S_N bond length (S_N = non-hydrogen-bonding sulfur) is 2.294 (2) Å, shorter by 0.034 Å than the average Co-S bond length of 2.328 (4) Å in the complex $[(C_6H_5)_4P]_2[Co(SC_6H_5)_4]$, in which hydrogen bonding is absent. The average Co-S_H bond length (S_H = hydrogen-bonded sulfur) in **1** is 2.320 (2) Å, equivalent to that in $[(C_6H_5)_4P]_2[Co(SC_6H_5)_4]$. More generally the average Co-$S_{(N+H)}$ bond length in **1**, 2.302 (1) Å, is 0.026 Å shorter than that of the non-hydrogen-bonding complex. These results suggest that a local stabilization of the $[Co(SC_6H_5)_4]^{2-}$ complex results from hydrogen bonding. Vibrational bands assigned to metal-ligand modes of approximate T_2 and A_1 symmetry are observed at 237, 231, 218, and 204 cm^{-1}, respectively, for **1** as compared with 235, 228, 220, and 201 cm^{-1} in $[(CH_3)_4N]_2[Co(SC_6H_5)_4]$, a non-hydrogen-bonding complex. The direction of the metal-ligand vibrational frequency shifts with hydrogen bonding is in agreement with X-ray crystallographic data. These results suggest that amide-cysteine hydrogen bonding may stabilize the iron-containing redox center in rubredoxin and thereby account for its relatively high redox potential.

Introduction

Hydrogen bonding between amide groups and cysteine sulfur is a feature of all iron-sulfur proteins.[1] Much of the importance of the N-H···S interaction derives from the fact that it may modulate the redox potentials of several of these proteins.[1,2] In rubredoxin (Rd), the $Fe^{2+/3+}$ redox couple occurs in the vicinity of -0.05 V, as determined by reduction in the presence of NADPH and NADPH-ferredoxin reductase.[3,4] Synthetic iron tetrathiolate complexes by contrast have redox potentials in the vicinity of -1.0 V versus SCE in organic media.[4,5-7] The most important factors that may account for differences in protein and model complex redox potentials are the high solvent dipole moment of water and amide-cysteine (N-H···S) hydrogen bonding in the protein. Positive redox potential shifts have been observed for iron(II) tetrathiolate complexes in micelles in aqueous solution,[2,8] which supports the idea of a solvent dipole moment influence. The redox couple of the $[Fe(S_2\text{-}o\text{-}xyl)_2]^{-2-}$ complex shifts from -0.99 V versus SCE in Me_2SO to -0.64 V in aqueous micelles. In the same environment the peptide complex[8] [Fe(*Z*-Cys-Pro-Leu-Cys-OMe)$_2$]$^{2-}$ exhibits a redox potential of -0.37 V versus SCE, very close to the potential observed in native Rd.[4] It has been suggested that this effect is, in part, due to favorable N-H···S hydrogen bonding to sulfur in a peptide sequence identical with that at the metal binding site of the protein.[8] In principle hydrogen bonding would decrease the crystal field at the metal center to a greater extent for the reduced rather than for the oxidized complex.

There has been a need for information in the study of hydrogen bonding in synthetic analogues of Rd. The present work addresses

† This work was presented in preliminary form at the 199th National Meeting of the American Chemical Society, April 22-27, 1990, Boston, MA.

(1) Adman, E. T. *Biochim. Biophys. Acta* **1979**, *549*, 107-144.
(2) Nakamura, A.; Ueyama, N. In *Metal Clusters in Proteins*; Que, L., Ed.; American Chemical Society: Washington, DC, 1988; Chapter 14.
(3) Lovenberg, W.; Sobel, B. E. *Proc. Natl. Acad. Sci. U.S.A.* **1965**, *54*, 193-199.
(4) Peterson, J. A.; Coon, M. J. *J. Biol. Chem.* **1968**, *243*, 339-334.
(5) Lane, R. W.; Ibers, J. A.; Frankel, R. B.; Holm, R. H. *Proc. Natl. Acad. Sci. U.S.A.* **1975**, *72*, 2866-2872.
(6) Lane, R. W.; Ibers, J. A.; Frankel, R. B.; Papaefthymiou, G. C.; Holm, R. H. *J. Am. Chem. Soc.* **1977**, *99*, 84-98.
(7) Moura, I.; Moura, J. J. G.; Santos, M. H.; Xavier, A. V.; LeGall, J. *FEBS Lett.* **1979**, *107*, 419-421.
(8) Nakata, M.; Ueyama, N.; Fuji, M.-A.; Nakamura, A.; Wada, K.; Matsubara, H. *Biochim. Biophys. Acta* **1984**, *788*, 306-312.

0020-1669/91/1330-2656$02.50/0